nature materials

REVIEW ARTICLE

PUBLISHED ONLINE: 6 SEPTEMBER 2009 | DOI: 10.1038/NMAT2496

Self-assembly and transformation of hybrid nano-objects and nanostructures under equilibrium and non-equilibrium conditions

Stephen Mann

Understanding how chemically derived processes control the construction and organization of matter across extended and multiple length scales is of growing interest in many areas of materials research. Here we review present equilibrium and non-equilibrium self-assembly approaches to the synthetic construction of discrete hybrid (inorganic–organic) nano-objects and higher-level nanostructured networks. We examine a range of synthetic modalities under equilibrium conditions that give rise to integrative self-assembly (supramolecular wrapping, nanoscale incarceration and nanostructure templating) or higher-order self-assembly (programmed/directed aggregation). We contrast these strategies with processes of transformative self-assembly that use self-organizing media, reaction–diffusion systems and coupled mesophases to produce higher-level hybrid structures under non-equilibrium conditions. Key elements of the constructional codes associated with these processes are identified with regard to existing theoretical knowledge, and presented as a heuristic guideline for the rational design of hybrid nano-objects and nanomaterials.

Nanoscale objects are the focus of much attention not only as critical components in the emergence of cellular life[1], but as small-scale materials with advanced functions and properties that can be isolated or assimilated into numerous applications, such as in bioelectronics, sensing, drug delivery, catalysis and nanocomposites[2–6]. In this review, we focus on hybrid nano-objects that are constructed by using organic components to coordinate the nucleation, growth, organization and transformation of inorganic nanophases to produce discrete integrated objects or higher-order structures under equilibrium or non-equilibrium conditions. Using illustrative examples, we systematize the concepts that underpin these assembly processes, and discuss theoretical considerations.

Integrative self-assembly

We begin by surveying present strategies used to coordinate the structure and organization of discrete hybrid nano-objects under equilibrium conditions[5,7]. These materials consist of inorganic nanocomponents, such as metals (Au, Ag), metal-ion salts ($Ca_3(PO_4)_2$, $CaCO_3$), quantum dots (CdS), magnetic (Fe_3O_4) and photoactive (TiO_2) oxides, and glassy solids (SiO_2), which are chemically integrated with discrete organic nanostructures. We classify the construction processes leading to single nano-objects as 'integrative self-assembly', and identify three systematic approaches: nanoscale incarceration, supramolecular wrapping and nanostructure templating (Fig. 1a–d).

Nanoscale incarceration. In general, hybrid nano-objects comprising entrapped inorganic components necessitate the pre-organization of persistent self-assembled organic architectures with hollow accessible interiors. An important archetype of this approach is the use and application of the capsid-like protein, apoferritin, for the controlled nucleation and confinement of inorganic nanoparticles[8]. Addition of various inorganic reaction mixtures under appropriate conditions (such as low concentrations, slow reaction rates, substoichiometric ratios and so on) has led to the synthetic construction of a wide range of novel protein-encapsulated core–shell hybrid nano-objects; most recently, these include ferritins with incarcerated nanoparticles of $CaCO_3$ (ref. 9), PbS (ref. 10), Ag (ref. 11) and In (ref. 12), as well as Pd (ref. 13) or CoPt (ref. 14) for use in catalytic hydrogenation and magnetic storage, respectively. Similar approaches have been developed using viral capsids[15–17]. In both systems, inorganic reactants permeate the polypeptide shell through molecular channels within the self-assembled architecture, and nucleation occurs specifically within the internal cavity. Although molecular diffusion into the ferritin cage is passive, pH-induced swelling of the shell of cowpea chlorotic mottle virus can be used to access the internal environment[16]. Interestingly, under certain conditions, the above protocols can be run in reverse such that preformed inorganic nanoparticles of appropriate size, shape and surface functionality can be used as platforms for the self-assembly of viral coat proteins[15] or apoferritin subunits[10]. For example, coat proteins assemble spontaneously around gold nanoparticles functionalized with anionic moieties, specific nucleic-acid packaging signals, or a monolayer of carboxy-terminated polyethylene glycol[18–20] (Fig. 2a).

Nanoscale incarceration of inorganic components within integrated hybrid objects can also occur under special conditions by confinement within lyotropic organic mesophases that are constrained in particle size. Although less common than cage-mediated entrapment, this process is intriguing as the hybrid nano-objects do not adopt core–shell architectures but instead have unusual mesostructured interiors. For example, quenching of synthesis mixtures of cationic amphiphiles and silicon alkoxides by rapid aerosol drying gives rise to the spontaneous co-assembly of spherical silica–surfactant nanoparticles with 'onion-like' internal architecture, in which the inorganic phase is incarcerated within a concentrically arranged lamellar mesostructure[21] (Fig. 2b). In contrast, rapid dilution and neutralization of analogous reaction mixtures produces oblate ellipsoidal nanoparticles of the hexagonally ordered silica–surfactant mesophase MCM-41, which have a highly unusual modulated mesostructure owing to structure-induced shape transformations during nucleation[22] (Fig. 2c).

Supramolecular wrapping. In this approach, supramolecular assemblies or macromolecules with well-defined persistent

Centre for Organized Matter Chemistry, School of Chemistry, University of Bristol, Bristol BS8 1TS, UK. e-mail: s.mann@bris.ac.uk

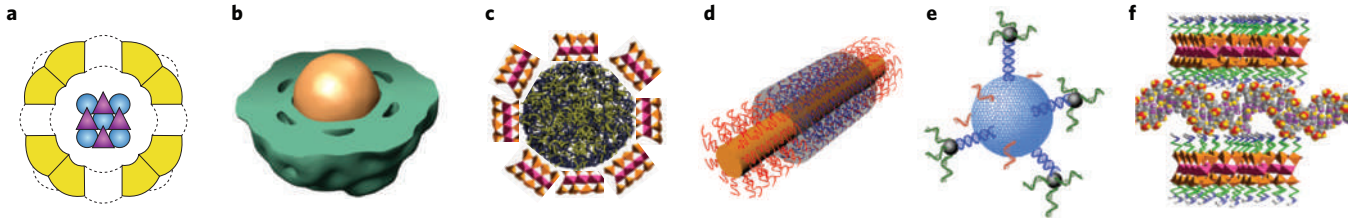

Figure 1 | Present approaches to the construction and organization of discrete hybrid nano-objects under equilibrium conditions. a–d, Integrative assembly. Nanoscale incarceration by confinement of inorganic reactions within preformed supramolecular organic containers (**a**), or by self-assembly of organic subunits around preformed inorganic nanoparticles (**b**). Wrapping of supramolecular organic nano-objects with ultrathin inorganic shells (**c**). Site-directed templating of inorganic components on organic nanostructures (**d**). **e**,**f**, Higher-order assembly of unitary nano-object constructs by programmed aggregation (**e**), and extended nanostructures by multicomponent reconstitution (**f**).

three-dimensional architectures are enveloped in a continuous inorganic coating under near-equilibrium conditions to produce discrete core–shell hybrid nanoparticles[23]. This approach is related to templating strategies (see below), but is differentiated by the continuous nature of the inorganic component and general absence of surface patterning. Sol–gel reactions, particularly those involving the hydrolysis and condensation of silica precursors, seem to be very compatible with high-fidelity wrapping. For example, organogel nanostructures have been successfully transcribed into silicified hybrids with cylindrical[24] or helical morphology[25], and similar procedures have been used to prepare silica-coated porphyrin-based nanotapes[26,27] and collagen fibrils[28].

Increasing attention is being placed on maintaining the functionality of the organic architectures after silica-shell wrapping to produce core–shell hybrids with integrated properties. Ideally, the organic functionality should be retained after assimilation of the inorganic component, and remain accessible to external stimuli such as changes in pH or optical excitation[27]. In practice, these triggers are transmitted to the embedded organic nanostructure through nanopores in the ultrathin silica envelope, thereby enabling collective functions to operate within a single hybrid nano-object. Significantly, these experimental protocols have been extended to the silica/organoclay wrapping of single molecules of polysaccharides[29,30], proteins[30–32], enzymes[31,33] and DNA[32] (Fig. 2d). In each case, the wrapped biomolecules remain structurally intact and maintain their functionality even under adverse conditions.

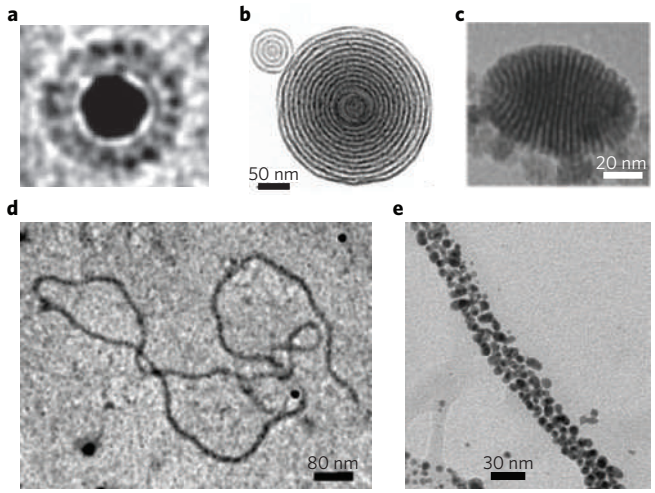

Figure 2 | Transmission electron microscopy (TEM) images of hybrid nano-objects produced by integrative self-assembly. a, Nanoscale incarceration of a single preformed gold particle by self-assembly of viral coat proteins[20]. **b**,**c**, Incarceration of SiO_2 within nanoparticles of ordered lyotropic surfactant mesophases showing interiors with concentric lamellae (**b**)[21], and a modulated hexagonal structure (**c**)[22], viewed side-on. **d**, Supramolecular wrapping of a single-plasmid DNA molecule in a continuous ultrathin shell of condensed organoclay oligomers[32]. **e**, Template-directed deposition of gold nanoparticles on the surface of a nanostructured tobacco mosaic virus rod-like particle to produce metallized biostructures with high shape anisotropy[34]. Figures reproduced with permission: **a**, © 2006 ACS; **b**, © 1999 NPG; **c**, © 2002 Wiley-VCH; **d**, © 2007 ACS; **e**, © 2008 RSC.

Nanostructure templating. A wide range of self-assembled organic architectures have been used as supramolecular templates for the construction of original hybrid nano-objects under equilibrium conditions. In general, slow reaction rates — aided by, for example, low levels of supersaturation and reactant concentrations — are used to facilitate favourable interactions specifically at the organic surface so that nanoscale inorganic deposition occurs preferentially along the accessible surfaces of the template (Fig. 2e). This site selectivity is improved in many cases by sequential exposure of the preorganized organic nanostructure to the individual inorganic reactants[34]. In practice, this often involves the substoichiometric binding of metal cations to the template surface, followed by adding ions/molecules that trigger inorganic deposition or crystallization. These procedures are particularly effective for the templating of metal or semiconductor nanoparticles within spherical objects such as dendrimer nanoparticles[35], or on the surface of highly anisotropic biological nanostructures such as DNA[36] and self-assembled microtubules[37]. Similarly, arrays of Au, Ag or Pt nanoparticles have been prepared by *in situ* deposition on the external or internal surface of rod-shaped tobacco mosaic virus particles[34,38,39]. As these hybrids are uniform in length and width, mechanically robust and accessible to physical manipulation, they may have important technological uses as components of digital memory devices[39] or as electrically conducting nanowires[40].

A diverse range of synthetic organic molecules has been used to prepare anisotropic nanostructures (such as filaments, tubes, helicoids and so on) that promote the template-directed assembly of integrated hybrid nanoscale objects under equilibrium conditions. Some representative examples include chiral lipids[41,42], peptide-based surfactants[43,44], block copolymers[45,46], dendron rod–coil triblocks[47,48] and T-shaped dendro-calixarene amphiphiles[49] (Fig. 3). Self-assembling peptides with sequences programmed to have appropriate polar or charged surface amino acid residues[50,51] that induce β-sheet (amyloid) formation[52,53], or initiate coiled-coil intermolecular interactions[54], have also been investigated. In many cases, these molecules self-assemble in water into nanostructured objects by enthalpic and entropic processes, and adopt highly anisotropic architectures because of the intricacies of molecular shape and size, and specificity of the intermolecular interactions.

In general, the above amphiphiles and peptides show certain key characteristics that are designed into the molecular structure to facilitate their use as effective templates for nanoscale inorganic

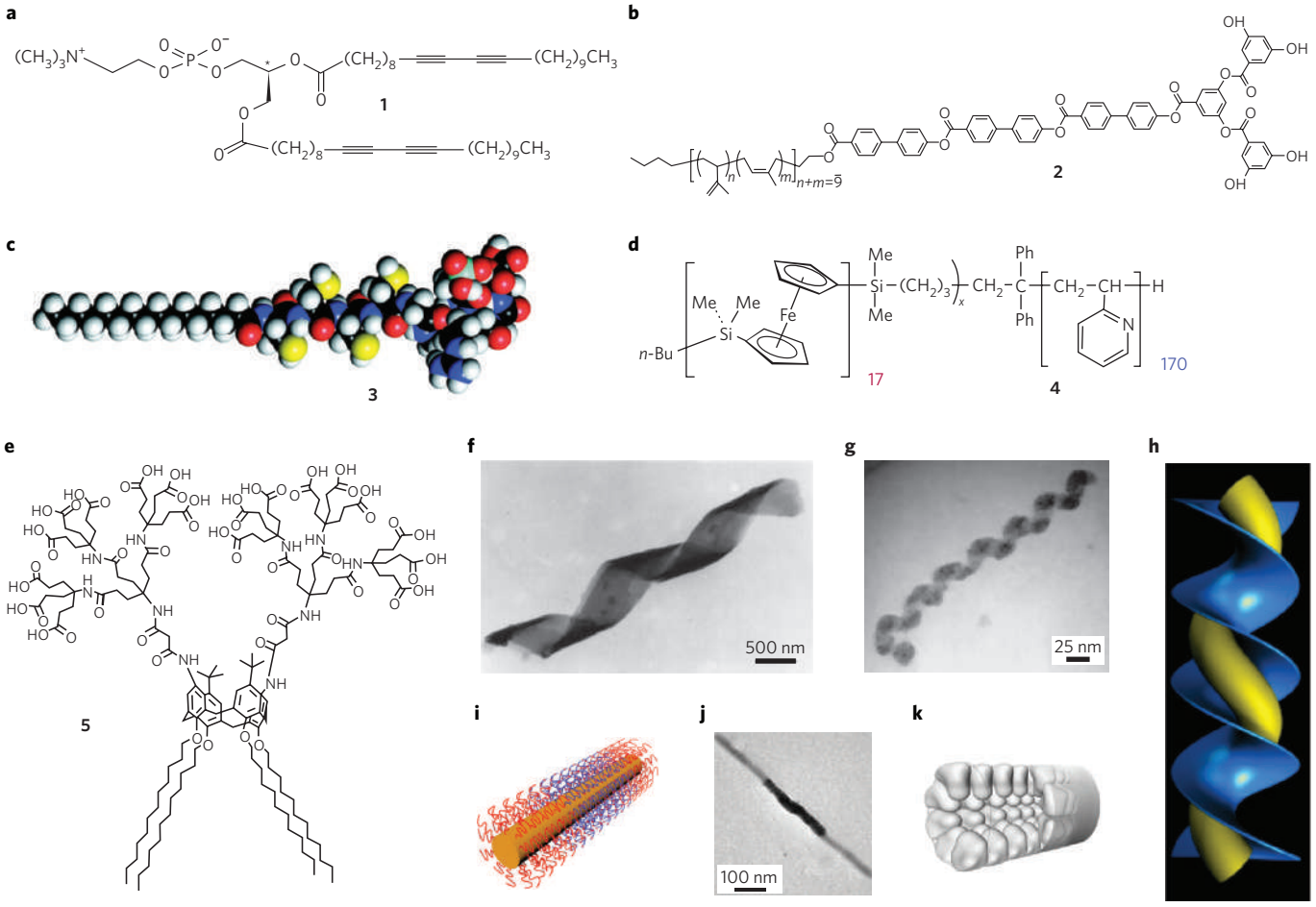

Figure 3 | Nanostructure templating of hybrid nano-objects. a–e, Examples of template molecules. **a**, Chiral phospholipid (**1**). **b**, Dendron rod-coil (**2**). **c**, Peptide-alkyl-chain surfactant (**3**). **d**, Diblock copolymer (**4**). **e**, T-shaped dendro-calix[4]arene (**5**) (see text for details). **f**, SiO_2 helicoid based on (**1**)[41]. **g**,**h**, CdS helicoid (**g**) based on (**2**), and corresponding graphic (**h**) showing templating of CdS on one surface of helicoid (**2**)[47]. **i**,**j**, Co-micelle of (**4**) with quaternized P2VP central region and unfunctionalized P2VP ends (**i**), and corresponding TEM image (**j**) showing patterned deposition of TiO_2 in the middle domain[46]. **k**, Graphic showing cut-away structure of a persistent cylindrical micelle formed from (**5**) with ordered surface corrugations of high negative charge[49]. Figures reproduced with permission: **a**,**b**,**g**,**h**, © 2002 Wiley-VCH; **d**,**j**, © 2009 Wiley-VCH; **e**, © 2007 Wiley-VCH.

deposition. For example, although phospholipid (**1**) (Fig. 3a) has a molecular structure closely related to that of conventional lipids, there are three features that make this amphiphile particularly useful as a template with programmed structure and embedded functionality. First, the zwitterionic headgroup provides flexibility in interfacial binding, such that anions (silicate)[41] or metal cations[42] can be sequestered preferentially at the headgroup surface. Second, the chiral centre positioned at the junction between the phosphocholine headgroup and acyl chains drives the molecular packing into a highly anisotropic twisted tubular architecture[55], which is retained in the hybrid counterparts (Fig. 3f). And third, positioning of the diacetylenic groups between C_8 and C_9 atoms promotes strong interchain interactions that structurally stabilize the bilayer motif, as well as facilitate UV-induced ene–yne chain polymerization to produce hybrid nano-objects with solvatochromic, thermochromic and mechanochromic properties[41].

Similar considerations have been applied in the design of the dendron rod–coil molecule (**2**) (Fig. 3b), which assembles into helical nanotapes by hydrogen bonding between the hydroxyl and carbonyl groups in the dendron segment and π-π stacking interactions of the aromatic rod domain[47]. Incubation of the twisted ribbons with $Cd(NO_3)_2$ in tetrahydrofuran, followed by reaction with H_2S, promotes nucleation of CdS nanocrystals specifically around the organic nanostructure to produce helically shaped nano-objects (Fig. 3g). Significantly, detailed investigations indicate that the CdS component is located on only one side of the twisted template (Fig. 3h), possibly because helicoids with a slightly coiled axis would have one face more exposed to the reactant molecules present in the solvent[48]. In other studies, nanoscale hybrid objects with desired biocompatibility are being developed by using peptide-based nanostructured templates in combination with inorganic components — such as $Ca_3(PO_4)_2$ and $CaCO_3$ — that mimic natural biominerals. For example, the peptide-alkyl-chain surfactant (**3**) (Fig. 3c) consists of three key engineered features in the headgroup region[44]: (i) four consecutive cysteine amino acids are included in the peptide sequence to generate disulphide bonds between adjacent molecules when self-assembled to produce robust nanofibres; (ii) a phosphoserine residue is included to promote binding of Ca^{2+} and subsequent site-directed nucleation of calcium phosphate; and (iii) the cell-binding motif Arg-Gly-Asp (RGD) is sited at the end of the headgroup to facilitate cell adhesion.

Complementary strategies based on block copolymer self-assembly are being developed for the template-directed construction of hybrid nano-objects with high shape anisotropy. For instance, cylindrical micelles prepared from poly(acrylic acid)-containing block copolymers have been used as organic templates for the formation of constructs comprising linear arrays of metallic, metal oxide or metal sulphide nanoparticles[56,57]. In a recent development,

the diblock copolymer, poly(ferrocenyldimethylsilane)-*b*-poly(2-vinylpyridine) (PFS_{17}-*b*-$P2VP_{170}$, (**4**) (Fig. 3d) has been used to prepare discrete cylindrical co-micelles that consist of a positively charged central region with a quaternized P2VP corona, along with un-functionalized end segments (Fig. 3i). The spatially defined coronal chemistries have been exploited for the localized nucleation of titania specifically across the central segment of each co-micelle[46] (Fig. 3j).

Although the above studies clearly demonstrate the success of nanostructure templating for the integrative self-assembly of hybrid nano-objects, the fidelity of transcription is usually low when viewed at sub-10-nm dimensions. This is because the surface charge distribution associated with packing of the amphiphilic molecules is generally homogeneous at this length scale, so there are no distinctive regions for site-specific inorganic nucleation or spatial confinement of the primary growth clusters. As a consequence, the inorganic components are nucleated randomly across the organic surface, and subsequently grow along the interface until they come into contact with each other. In principle, these limitations can be circumvented by using a sterically constrained bulky amphiphile with a sufficiently rigid molecular geometry to produce packing arrangements that impose structurally persistent binding domains across the surface of the template. A possible archetype of this system is the self-assembly of the T-shaped dendro-calix[4]arene amphiphile (**5**) (Fig. 3e) into structurally rigid micelles with regularly arranged 2.5-nm-wide surface corrugations lined with several carboxylate ligands[58] (Fig. 3k). In this case, the high negative charge density within these surface domains is sufficient to restrict the nucleation and growth of CdS clusters to the corrugated regions, such that quantum dots are organized as discrete components along the cylindrical micelle[49].

Higher-order equilibrium self-assembly

The considerable difficulties associated with achieving high-resolution spatial separation and organization of individual components within single nano-objects prepared by *in situ* deposition (integrative assembly) can be alleviated to some extent by using preformed nanostructured components that undergo spontaneous higher-order assembly under equilibrium conditions to produce unitary nano-objects or extended nanostructutures (Fig. 1e,f). In each case, the extent of constructional ordering and component placement is dependent on the level of interparticle specificity encoded into the individual building blocks.

Unitary nano-objects. Co-organization of two or more types of particles within the same nanoscale object is attracting much attention as a route to preparing dispersed nano-objects with multifunctionality. Typically, this involves conjugation of spherically shaped particles of different size and composition, with the larger component acting as a central platform to control the coupling of the smaller constituents to produce a unitary nano-object with satellite-like organization[59] (Fig. 4a). Interparticle specificity is often achieved by ligation of complementary organic molecules to the different nanoparticle surfaces, such that the components are assembled into persistent arrangements by molecular recognition. This strategy of 'programmed aggregation' often involves biomolecular-induced interparticle coupling, and is related to pioneering work on the DNA-induced assembly of gold nanoparticles into disordered networks[60]. Similar approaches using high-affinity non-covalent recognition between streptavidin/biotin or antibody/antigen conjugates have been developed to construct a range of multicomponent, biologically active nanoscale hybrid objects[61]. As the coupling interactions are reversible and highly selective, the encoded nano-objects can be assembled and disassembled by changes in temperature and ligand concentrations.

The programmed assembly of nanoscale objects from components of different size and shape seems to be a promising approach to a range of new multifunctional nanostructures with ordered constituents. Several approaches have been investigated based on the use of biomolecular, covalent or electrostatic binding. For example, oligonucleotide-capped gold nanoparticles and protein-coated iron oxide nanoparticles (ferritin) have been assembled on the surface of individual carbon nanotubes (CNT) to produce constructs with optical, superparamagnetic and metallic/semi-conductive properties[62]. As the coupling interactions between the gold and protein molecules are dependent on biotin/streptavidin linkages and duplexation, addition of excess biotin or thermal treatment results in disassembly specifically of the gold nanoparticles (Fig. 4b), as well as subsequent changes in function that might be exploited in bioelectrochemical and biosensing applications. An intriguing example of reversible assembly triggered by conformational changes, rather than by biomolecular decoupling, is the stabilization and release of a single CdS guest nanoparticle from the open-ended cylindrical cavity of a barrel-shaped chaperonin protein complex[63] (Fig. 4c).

Other studies have used covalent coupling to addressable amino acids to prepare biologically derived hybrid nano-objects from nanostructured components of different size and shape. For example, gold nanoparticles have been assembled onto amyloid-like fibres genetically engineered with surface-accessible cysteine residues[64], tagged with surface Ni-NTA groups (NTA = nitrilo-triacetic acid) and positioned specifically within the 11 nm ring of the heat-shock protein complex, SP1, by high-affinity binding to six localized histidines[65], or functionalized with hydroxyl–succimido ligands for assembly onto collagen-like peptide fibres containing a designed sequence of lysine residues[66]. Significantly, high levels of definition in the placement of gold nanoparticles can be achieved by exploiting the underlying spatial arrangement of the coat proteins of viral capsids. For example, preformed gold nanoparticles are assembled at specific locations around the external surfaces of cowpea mosaic viral particles by genetically engineering cysteine residues at symmetry-related positions in the icosahedral cage[67]. Although this level of fidelity is difficult to emulate in non-biological nanoscale objects, recent studies have indicated that synthetically derived nano-objects can be patterned by electrostatic interactions during co-assembly of the constituent units. For example, the addition of carboxylate-functionalized gold nanoparticles to poly(ferrocenyldimethylsilane)-*b*-poly(2-vinylpyridine) (**4**) (Fig. 3d) co-micelles, which consist of a central positively charged segment, results in spatially patterned hybrid nanocylinders due to charge matching between the nanoscale components[45] (Fig. 4d).

Finally in this section, we note that unitary nano-objects can be produced spontaneously by the self-assembly of a single nanoscale component with a composite hybrid substructure. For example, 2-nm-sized gold nanoparticles functionalized with reactive maleimido groups have been coupled specifically to an exposed cysteine residue of the engineered β-subunit of the chaperonin HSP60, and the hybrid construct used for the spontaneous self-assembly of a hollow double-ring nanostructure with spatially ordered gold nanoparticles[68] (Fig. 4e). This approach is facilitated by strong subunit–subunit interactions that drive the system enthalpically and entropically towards the higher-order structure. Clearly, the nanoparticles have to be small enough to be physically accommodated within the integrated architecture, so consideration of the size ratio of the components is an important criterion. A similar strategy has been demonstrated by attaching gold nanoparticles to F-actin subunits before self-assembly of spatially patterned Au/actin nanofibres[69].

Extended nanostructures. The formation of extended networks by interparticle conjugation between fluid-dispersed hybrid nanoparticle building blocks is facilitated by electrostatic, steric, van der Waals, hydrophobic and dipole–dipole interactions[70]. The simplest situation involves the spontaneous assembly of weakly

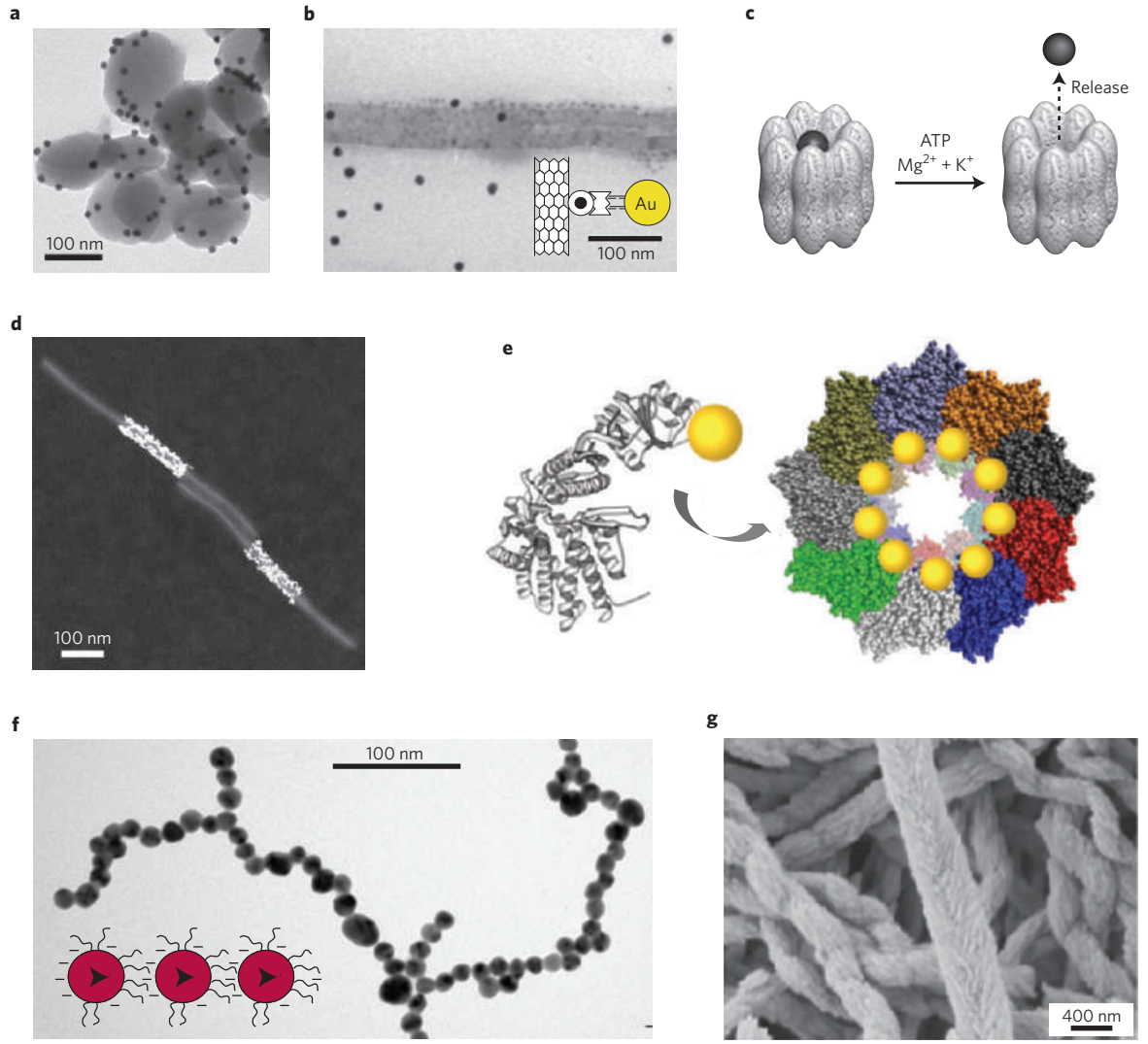

Figure 4 | Higher-order assembly of nanoscale hybrid objects. a–e, Self-assembly of unitary nano-objects. **a**, Programmed aggregation based on DNA-directed attachment of gold-nanoparticle satellites to single nanoparticles of mesoporous silica[59]. **b**, Coupling of oligonuceotide-functionalized gold nanoparticles to ferritin molecules adsorbed onto the surface of a CNT through a streptavidin linker[62]. The TEM image shows the specific disassembly of the gold nanoparticles (imaged as larger dark dots) by heat-induced dehybridization of the DNA linkages. The iron oxide cores of ferritin (smaller, less-dense spots) remain firmly attached to the CNT platform. **c**, Scheme showing triggered release of a single semiconductor nanoparticle from a chaperonin–CdS nanoconstruct[63]. **d**, Patterned electrostatic assembly of gold nanoparticles on individual block-copolymer cylindrical co-micelles of (**4**). **e**, Scheme showing self-assembly of a gold/chaperonin ring-shaped architecture from gold-nanoparticle-tagged protein subunits[68]. **f**,**g**, Higher-order extended structures. **f**, TEM image showing spontaneous assembly of linear chain of spherical gold nanoparticles with branching bifurcations[77]. The graphic illustrates dipolar interactions associated with ligand partitioning on the gold nanoparticle surfaces. **g**, Mesocrystal of $BaCO_3$ showing helical stacking of iso-oriented crystals produced by selective adsorption of a phosphonated double hydrophilic poly(ethylene oxide-oxabutylacrylate ester) block copolymer onto the (110) face of the nanocrystals during aqueous precipitation[91]. Figures reproduced with permission: **a**, © 2005 Wiley-VCH; **b**, © 2005 RSC; **c**, © 2003 NPG; **d**, © 2007 ACS; **e**, © 2002 NPG; **g**, © 2005 NPG.

or non-interacting spherical nanoparticles, which produces close-packed, high-symmetry arrangements, typical of many colloidal nanocrystals prepared by evaporation-induced assembly from organic solvents containing hydrophobically functionalized inorganic nanoparticles[2,3]. The hydrophobic and near-contact van der Waals attractive energies are proportional to $e^{-d/\lambda}$ and $1/d$ respectively (d = distance between surfaces, λ = 1–2 nm)[70]. Moreover, high perfection in lattice ordering demands stringent levels of uniformity in particle size and shape, which are often difficult to achieve synthetically. Interestingly, incarceration of inorganic nanoparticles in spherical capsid-like architectures (for example, ferritin, cowpea brome mosaic virus) can circumvent problems associated with polydispersity of the inorganic phase, as well-defined molecular interactions between the protein shells override the imperfections to produce very accurate placement of the hybrid nanoparticles[71].

Deviations from close packing of spherical nanoparticles can be accomplished under certain conditions — for example, low-density diamond-like lattices have been assembled from strongly electrostatically interacting spherical nanoparticles in the presence of counter-ion screening effects[72], where the attractive/repulsive energies scale proportionally with $e^{\kappa/r}$ (r = distance between ions, κ^{-1} = screening length)[70]. However, it is generally true that increased levels of organization in nanoparticle-based higher-level structures require interparticle specificity and directionality. Specificity is increased considerably in systems comprising spherical nano-objects by programmed aggregation using DNA-based coupling with appropriate design of biomolecular linkers and thermal pathways[73,74].

Alternatively, higher-order arrays of hybrid nano-objects with considerable spatial directionality can be constructed by exploiting interparticle dipole–dipole interactions. Significantly, when these interactions are dominant over competing interparticle forces — for example, for particles with considerable intrinsic magnetic[75] or electric dipoles[76] — then one-dimensional linear chains of isometric nanoparticles self-assemble spontaneously in the dispersed medium. Chain assembly can be facilitated also by modifications in the hybrid nature of the nanoparticles. For example, reducing the screening effect of the organic stabilization layer that surrounds spherical CdTe semiconductor nanoparticles promotes linear chain aggregation owing to increases in the interparticle electric dipole–dipole interactions[76]. Unlike semiconductor quantum dots, face-centred-cubic metallic nanoparticles show no intrinsic electric dipole, yet gold nanoparticles spontaneously assemble into linear arrays when conjugated with several types of surface-attached ligands[77,78] (Fig. 4f). Clustering of the organic molecules into discrete domains on the inorganic surface produces an extrinsic electric dipole that is sufficient to align the nanoparticles through cumulative dipolar interactions to produce linear chains and networks showing plasmonic coupling[6,77].

In contrast to spherical nano-objects, the construction of spatially aligned higher-level superstructures from components with considerable shape anisotropy, such as nano-sheets and nanorods, is inherently directional owing to entropic ordering[79]. As a consequence, nanoparticles such as hydrophobically stabilized Au (ref. 80), Co (ref. 81) or $BaCrO_4$ (ref. 82) nanorods will spontaneously self-assemble into linear chains by side-on ordering. The ordering process is further enhanced by enthalpic processes related to intermolecular interactions between the surface-adsorbed surfactant molecules on the side faces of neighbouring nanoparticles. These can result, for example, in the formation of an interdigitated bilayer between adjacent particles in the assembled superstructure, particularly if the nanorods have well-defined crystal faces[82]. Recent studies have developed this concept by attaching polystyrene molecules specifically to the end faces of surfactant-coated gold nanorods[83]. Similarly, enthalpy-driven interactions are often used for the spontaneous assembly of ordered mesolamellar structures from dispersions of hybrid nanosheets. For example, electrostatic interactions between dispersed polymer-stabilized graphene sheets have been used to promote the assembly of novel nanostructures in the form of electrically conductive thin films[84] and DNA-intercalated bio-nanocomposites[85].

Mesocrystals. The above examples consider systems of higher-order equilibrium assembly of spherical or anisotropic hybrid nano-objects, in which the inorganic-based building components are intrinsically stable with respect to structural transformation and interparticle fusion. There are however, a growing number of reports of non-classical crystallization processes involving the oriented attachment and partial fusion of nanoscale hybrid units[86], which result in the formation of mesocrystals that are crystallographically continuous and morphologically well-defined in three dimensions[87]. These crystals consist of an iso-oriented higher-order superstructure of coherently interconnected nanoscale inorganic domains with intercalated organic constituents — usually in the form of water-soluble polymers — that together significantly influence both the texture and mechanical properties. Mechanistically, binding of the organic macromolecules to crystal faces of the primary inorganic nanoparticles produces hybrid conjugates with shape and surface modifications that promote coordinated aggregation of the superstructure with high levels of orientational, but not positional, order[87–90]. Remarkably, the latter can be strongly influenced by macromolecular encoding of a subset of the crystal faces of the primary nanoparticles, with the consequence that non-geometric forms such as helical microstructures are spontaneously propagated by vectorial aggregation[91] (Fig. 4g).

How the nanocrystalline subunits attain such high levels of alignment is not known. However, it seems likely that the interplay between the minimization of the nanoparticle surface energy by fusion and coherent extension of the crystal lattice, and the steric-repulsion energy associated with the adsorbed polymers in the confined medium, is an important factor in this coordinated process of alignment. As the steric-repulsion energy is proportional to $e^{-d/R}$ (R = radius of gyration)[70], both polymer structure and packing density within the aggregates at the early stages of their formation must be important considerations. Furthermore, polarization forces and dipole fields have been proposed as mechanisms for mediating the alignment process[92,93]. As these competing forces are operating under near-equilibrium conditions, the perturbations caused by the ordering process are minimal and locally confined. In contrast, major structural modifications might be expected if the aggregated nanoparticle subunits and organic constituents are metastable and coupled through *in situ* phase transformations. This and other examples of non-equilibrium self-assembly involving nanoscale hybrid building blocks are discussed in the following sections.

Transformative self-assembly

The prescriptive nature of equilibrium-based strategies of integrative self-assembly limits the versatility to which multiple length scales and higher-order complexity can be embedded within the resulting hybrid constructs. In contrast, divergent pathways of construction involving nano-objects that undergo spontaneous ordering or transformation across several length scales can result in complex hierarchical states[88]. We classify these processes as 'transformative self-assembly' to distinguish their nonlinearity and emergent behaviour from mechanisms of higher-order self-assembly operating under equilibrium conditions. Three systematic approaches involving self-organizing media, reaction–diffusion systems or coupled-mesophase transformations, are highlighted below.

Nanoscale ordering in self-organizing media. Many non-equilibrium systems spontaneously transform into complex patterns and forms because of instability thresholds associated with spatio–temporal gradients in temperature, pressure, viscosity and chemical potential[94]. Some of these processes, such as viscous fingering, diffusion-limited aggregation, myelination, vortexation and foam generation, produce self-organized media that in principle could be exploited for the non-equilibrium self-assembly of inorganic nano-objects into materials with spatial patterns and complex morphologies. For example, sol–gel reactions have been coupled with the spontaneous formation of myelin-like tubular structures of the diblock copolymer amphiphile, poly(ethylene oxide)-*b*-poly(1,2-butylene oxide)[95]. The myelin outgrowths, which are metastable intermediates between the gel-like lamellar phase and dispersed multilamellar vesicles, are trapped in the form of highly anisotropic silica–polymer hybrid nanotubes by the addition of tetraethoxysilane to the polymer gel before immersion in water (Fig. 5a). As a consequence, chaotic outgrowth of the multilamellar myelin filaments is concurrent with silica deposition at the polymer/water interface to produce mineralized replicas of the emergent nanostructures.

Other studies have exploited microphase partitioning to enforce the spatial confinement and organization of nanoscale objects. For example, a wide range of hierarchically organized monolithic materials (for example, SiO_2, V_2O_5 and TiO_2) have been produced using air–liquid foams in association with sol–gel chemistry[96,97]. In many cases, the scaffold walls consist of coherently packed inorganic nanoparticles and are often porous across a range of length scales. Significantly, changing the drainage properties of the foams by altering the their liquid fraction results in modifications in the curvature and dimensions of the plateau border, which in turn influence the shape and size of the self-organized polygonal framework. A similar approach, in which viscous dextran gels containing metal salts or

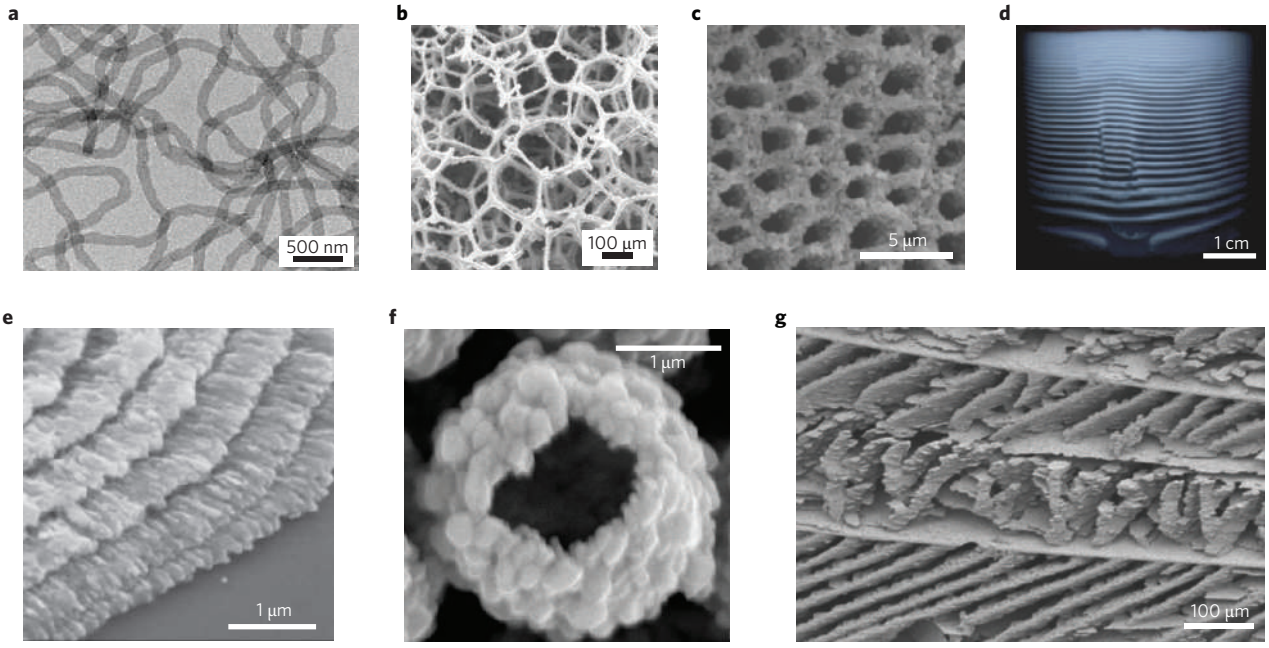

Figure 5 | Non-equilibrium spontaneous assembly of hybrid nanostructures. a,**b**, Use of self-organized media. TEM image showing SiO_2–polymer nanotubes formed by myelination of poly(ethylene oxide)-*b*-poly(1,2-butylene oxide)–tetraethoxysilane gel particles in water (**a**)[95], and scanning electron microscopy (SEM) image showing a polyhedral framework of zeolite and SiO_2 nanoparticles produced by microphase separation and spatial patterning within the interstitial voids of a dextran-derived foam of CO_2 gas bubbles (**b**)[98]. **c**–**g**, Examples of reaction–diffusion systems in higher-order self-assembly of nanostructures. **c**, Hierarchically ordered TiO_2 produced by non-equilibrium sol–gel reactions. The SEM image shows the cross-section of the internal structure of a macroscopic TiO_2 fibre comprising a de-mixed arrangement of ordered capillaries and nanostructured walls[106]. **d**, Optical image showing macroscopic ordering of iron oxide (white rust) in agar gel produced by diffusion–reaction precipitation of Fe(II)/Fe(III) under the influence of a pH gradient (reproduced with permission from www.damtp.cam.ac.uk/user/gold/research.html). **e**, SEM image showing periodic patterning of oriented calcium carbonate (calcite) nanoscale needle-like crystals in a spin-coated hydrogel of cholesterol-functionalized pullulan containing poly(acrylic acid). The bands are about 0.8 μm in width, and the calcite crystals are aligned along the crystallographic *c* axis[112]. **f**, SEM image showing a partially broken $CaCO_3$ hollow microsphere prepared by spontaneous self-transformation at 70 °C and pH 10.5 in the presence of poly(styrene sulphonate). The shell wall consists of vaterite nanocrystallites[115]. **g**, SEM image of a hierarchically ordered K_2SO_4 superstructure produced by evaporation-induced crystallization in the presence of poly(acrylic acid). The image shows the macroscopic scaffold constructed from the episodic deposition of plates interspaced with polycrystalline columns of K_2SO_4 crystallites[117]. Figures reproduced with permission: **b**, © 2004 Wiley-VCH; **e**, © 2003 Wiley-VCH; **g**, © 2005 Wiley-VCH.

inorganic nanoparticles are decomposed into foams under slow thermal processing has been recently reported[98] (Fig. 5b).

Reaction–diffusion systems. Diffusion-limited reaction fronts comprising spatially and temporally coupled chemical gradients have been reported for a wide range of non-equilibrium phenomena[99]. In general, pattern formation depends on the competition and delicate balance between reaction and diffusion, and can be described mathematically by a set of partial differential equations that account for the spatio–temporal distribution of concentrations in open and closed nonlinear systems[100]. Significantly, the resulting concentration patterns may become fixed in time and space to produce persistent structures with complex organization[101–105]. Thus, it seems feasible that reaction–diffusion structures could be used in numerous systems to organize nanoscale components into patterned arrangements not readily accessible by equilibrium processes. For example, several studies have demonstrated that patterned arrangements of interconnected inorganic nanoparticles can be spontaneously produced by injecting a liquid metal alkoxide into aqueous ammonium hydroxide (Fig. 5c)[106–108]. The studies indicate that the ordering process is dependent on the spontaneous formation of a thin semi-permeable metal oxide membrane at the alkoxide/water interface, followed by subsequent spatio–temporal patterning of the nanoparticulate product by microphase separation along the diffusion-limited reaction front.

It is well established that time- and spatial-dependent oscillations in reactant concentrations and conditions are accentuated when supersaturated solutions are contained within viscous media such as silica or polymer hydrogels, and that such systems produce macroscale precipitation patterns often with banded or periodic organization[109,110] (Fig. 5d). Grzybowski and colleagues have exploited this process to prepare planar materials with spatial gradients, multicolour nanopatterns and multilevel surfaces by using agarose stamps to transfer a reactant solution into films of dry gelatine doped with a co-reactant[99]. Such materials have been developed as prototypes for static sensing, for example to detect changes in molecular configuration by modifications in the mass-transfer properties of thin gelatin films[111].

Significantly, recent studies have shown that many of the long-range patterns produced in viscous polymer gels are constructed from the hierarchical ordering of nano-sized particles and crystallites[112–114]. Organization of the nano-objects within the viscous environment is dependent to a large extent on the interplay between internal forces (crystallization) and external fields associated with diffusion–precipitation fronts that propagate through the system. The studies indicate that these factors are strongly influenced by the morphology and chemical activity of the system. For example, radial patterns comprising regular bands of crystallographically ordered $CaCO_3$ nanocrystallites are predominant in thin hydrogel films containing poly(acrylic acid) (PAA) owing to the continuous nature of the reaction medium[112] (Fig. 5e), whereas crystallization of amorphous $CaCO_3$ particles in the presence of poly(styrene sulphonate) produces hollow microspheres by spontaneous redistribution of matter from the interior to the outer surface[115] (Fig. 5f). In the latter

system, construction of the nanostructured polycrystalline shell at the expense of the amorphous core occurs by time-dependent decreases in supersaturation that allow crystallization of the porous outer shell and dissolution of the metastable core to be spatially and temporally coupled[116].

There is growing evidence that the spontaneous organization of nanoscale components into superstructural arrangements is often promoted in diffusion-limited reaction media by the addition of auxiliary polymers or surfactants to the viscous gel; this suggests that polymer–crystal interactions between hybrid nano-objects are of significant mechanistic importance in generating divergent pathways of construction under non-equilibrium conditions. For example, six levels of embedded structural order have been demonstrated within a complex macroscopic scaffold by controlling the concentration of PAA in aqueous solutions of K_2SO_4 subjected to slow evaporation at 25 °C (Fig. 5g)[117]. The architecture consists of layers of K_2SO_4 plates interspaced with columns that are constructed from stacks of micrometre-thick sheets, which in turn are built from the iso-oriented assembly of K_2SO_4/PAA hybrid nanocrystals. Each level of organization reflects different outcomes of the interplay between cooperative and competitive growth processes, which are mediated by oscillations in the local supersaturation and PAA concentration. Together, these determine the nature of the constructed hybrid structures by regulating crystallization along either two or three dimensions.

Structural morphogenesis. As well as controlling the aggregation behaviour of crystalline nanoparticles, polymers and surfactants can have a key role in promoting the nucleation of metastable nanoparticles, as well as mediating their subsequent transformation into more stable structures. Typically, this involves transformation of amorphous states or metastable polymorphs into crystalline counterparts. Significantly, under non-equilibrium conditions, these transformations may become coupled with local fields and gradients to produce hybrid nanostructures with hierarchical organization and complex form. For example, numerous higher-order structures have been reported for inorganic-precipitation reactions in water-in-oil microemulsions or polymer-containing aqueous solutions, and several of the underlying mechanisms have been discussed[88].

In general, transitions from the isotropic (amorphous) to anisotropic (crystalline) state under local non-equilibrium conditions are critically important as they result in the breaking of the symmetry that is necessary for the propagation of divergent constructional pathways. These mesoscale transformations occur within the confined fields of metastable colloidal aggregates that initially consist of loosely packed, amorphous inorganic nanoparticles and relatively high concentrations of surface-adsorbed organic molecules[118]. Dipolar interactions between the metastable nanoparticles, as well as rearrangements in the surface-attached organic molecules, mediate the transformation pathways to produce highly anisotropic single-crystal nanofilaments or nanoplates. As these structures are also highly unstable, they tend to aggregate into co-aligned stacks[119], or become structurally modified. In the latter case, the system either reverts to thermodynamic equilibrium, with the consequence that the filaments are transformed into geometrically shaped nanoparticles or short nanorods with increased crystallinity[120], or they become interlocked into new non-equilibrium emergent architectures in the form of bundles of highly elongated crystalline nanofilaments[118]. Initially, the bundles consist of loosely packed nanowires, but with time, crystalline contacts are formed at local regions between adjacent filaments, such that the nanofilaments become co-aligned and crystallographically coherent (Fig. 6a,b). However, as the interfilament contacts are entropically frustrated by the presence of the surface-adsorbed organic molecules, only localized regions are crystallographically continuous, with the consequence that positional disorder and accumulation of defects in the bundles produces excessive lateral strain. This leads to new types of instability and further symmetry breaking in the construction process. In particular, strain-induced bending and folding of the soft hybrid nanostructures result in coiling of the bundles into spirals that subsequently propagate into complex, hierarchically organized micro- and macroscale objects (Fig. 6c).

The above observations indicate that structural morphogenesis of nanoscale hybrid objects across several length scales can be achieved spontaneously through a series of instability thresholds. These thresholds derive initially from chemically based processes of kinetically controlled nucleation and disorder-to-order mesoscale

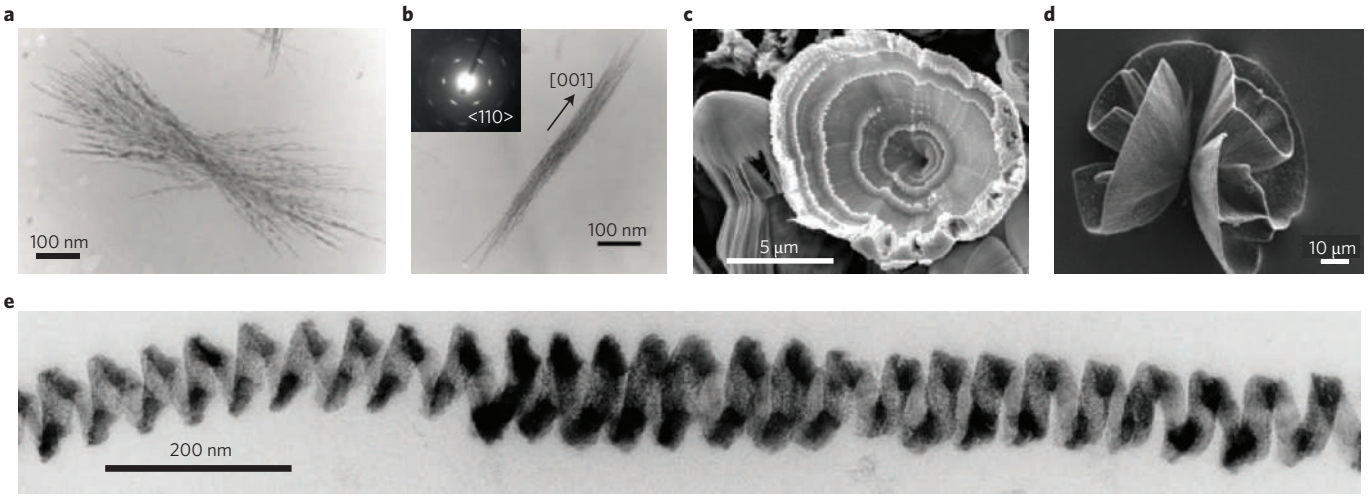

Figure 6 | Structural morphogenesis of hybrid nano-objects into higher-order forms under non-equilibrium conditions. a,**b**, TEM images of $BaWO_4$ nanofilaments produced in water-in-oil microemulsions (S. M., C. J. Johnson, unpublished results); initial stage of mesoscale aggregation showing loose bundle of nanofilaments (**a**), and later stage displaying rigid bundle with crystallographically co-aligned nanofilaments (**b**). Inset shows electron-diffraction pattern from the bundle viewed down the <110> zone, indicating that the nanofilaments are oriented along the [001] axis. **c**, SEM image of a $BaSO_4$ cone-shaped microstructure prepared in water in the presence of a phosphonated poly(ethylene-methylmethacrylate) hydrophilic block copolymer. The self-similar structure is generated from the spontaneous assembly of splayed bundles of $BaSO_4$ nanofilaments[118]. **d**, SEM image showing folded SiO_2–$CaCO_3$ coralline-like biomorph produced in alkaline SiO_2 sols[114]. The folded walls consist of ordered nanocrystallites of $CaCO_3$. **e**, TEM image showing a single helical nanofilament of crystalline $BaSO_4$ produced in water-in-oil microemulsions[125]. Figures reproduced with permission: **c**, © 2004 RSC; **d**, © 2008 ACS.

transformations, followed by collective phenomena related to the anisotropic build-up and dissipation of mechanical stresses associated, for example, with positional disorder, packing forces, dehydration, crystal defects and elasticity. These higher-order transformations represent a balance between competing processes, and seem to be dependent on stochastic fluctuations in shear, bending and hydrodynamic forces. Similar processes have been implicated in the patterning of microcrystals in hydrogel–polymer films[121], rolling and folding of supramolecular objects into hierarchical objects[122], enhanced folding in SiO_2–$CaCO_3$ biomorphs[114,123] (Fig. 6d), selection of different pathways in the hierarchical assembly of helical J-aggregate microstructures[124], and helical twisting of $BaSO_4$ nanofibres[125] (Fig. 6e).

Towards constructional codes for nanoscale objects

This review has surveyed recent approaches to the synthetic construction of discrete nano-objects, and their spontaneous ordering and transformation under equilibrium or non-equilibrium conditions. In this final section, the key elements associated with the constructional codes underpinning these different routes are identified with respect to existing theoretical knowledge, and offered as a heuristic guideline for the design of such systems. We classify these codes according to whether the associated construction pathways are commensurate (convergent) or incommensurate (divergent) with regard to the length scales of the principal building blocks.

Convergent pathways, such as integrative self-assembly, are prevalent under equilibrium conditions, although non-equilibrium processes can also operate in this mode[126]. Typically, approaches based on nanoscale incarceration, wrapping or templating are critically dependent on the interplay of two main engines of construction — organic self-assembly and inorganic nucleation — both of which are informed by equilibrium-based constructional codes with properties that specify various outcomes and processes, such as supramolecular pre-organization of the organic nanoscale architectures and interfacial complementarity in site-directed inorganic nucleation (Table 1). Pre-organization of organic nanostructures, such as block-copolymer micelles, polypeptide cages and virus capsids, can be described by existing theories of equilibrium self-assembly that highlight the importance of both enthalpic and entropic processes in attaining free-energy minimization[127]. In this respect, interactions associated with intermolecular bonding (electrostatic, hydrogen bonding, van der Waals, dipole–dipole, aromatic π-π and so on)[70], as well as contributions from molecular packing constraints, interfacial curvature, and matching of surface amphiphilicity and charge[128], are of central importance. These interactions have different magnitudes and scalar properties (proportional to $1/r$, $1/r^2$, $1/r^3$ and $1/r^6$ for electrostatic, hydrogen bonding, dipole-dipole and van der Waals interactions, respectively[70]; r = intermolecular distance), and are encoded within the design of the molecular structure (see 'Nanostructure templating' section for illustrative examples of amphiphile design). As a consequence, organic supramolecular self-assembly is regulated principally by internally derived information that is highly prescriptive and persistent, and collectively described by the initial state of the system.

Besides structural codes, there are extra levels of information that are required to specify the functional properties of pre-organized organic architectures as progenitors of hybrid nanoconstructs. For the most part, these concern the efficacy of the organic structures to direct inorganic nucleation and growth specifically within or along the supramolecular architecture. This critical dependence on interfacial complementarity is analogous to many biomineralization processes, in which the activation energy for inorganic nucleation is lowered through a variety of mechanisms such as metal-ion binding and clustering (iontropy), structural matching (epitaxy) and stereochemical correspondence[129]. Each of these mechanisms is dependent on the nature of the ligands exposed at the organic surface and their spatial arrangements, which in turn are encoded in molecular structure and packing considerations. In many synthetic and biomimetic systems, the localized accumulation of metal cations on the organic surface seems to be the predominant mechanism for lowering the interfacial energy associated with inorganic nucleation. For instance, studies on the fabrication of metallized protein nanofilaments indicate that histidine residues are prominent sites for Pt(II) or Pd(II) binding[37], whereas Au and Ag salts are sequestered specifically by cysteine residues[130]. As a consequence, there have been several reports on the preparation of hybrid nanostructures using synthetic peptide nanostructures with specifically designed binding domains[50–52], and incorporation of lysine residues into collagen-like peptide fibres has been used to promote gold-nanoparticle attachment[66]. Moreover, new types of protein-based hybrid nanoscale objects can be designed by introducing appropriate site-directed modifications by genetic engineering. For example, nucleation of iron oxide within the internal cavity of cowpea chlorotic mottle virus is promoted specifically by replacing lysine residues in the capsid interior with glutamic acid side chains that sequester Fe(II) ions from the external medium[131]. Similarly, genetically engineered ligation of a Ag-binding/reduction dodecapeptide to the C-terminus of the apoferritin subunit has been used to prepare protein-encapsulated silver nanoparticles[11].

Table 1 | Constructional pathways to hybrid nano-objects, networks and extended nanostructures.

Properties	Encoded processes	Outcomes
Convergent pathways (equilibrium): integrative self-assembly / higher-order assembly		
Prescriptive	Supramolecular preorganization	Nanometre length scales
Initial-state dependent	Site-directed inorganic nucleation	Intermediate complexity
Scalar equivalence	Interfacial complementarity	Quasi-geometric forms
Non-additive	Mesocrystal assembly	Unitary nano-objects
Persistent	Biomolecular recognition	Reversibility
	Interparticle interactions	Extended networks
Divergent pathways (non-equilibrium): transcriptive self-assembly		
Non-prescriptive	Diffusion-limited reaction fronts	Multiple length scales
System-generated	Microphase partitioning	High structural complexity
Propagation in time/length	Mesoscale transformations	Complex forms
Additive	Instability thresholds	Patterning
Competitive	Symmetry breaking	Irreversibility
	Stress/shear-induced transitions	Hierarchy

In contrast to the above processes, non-equilibrium processes of higher-order nanoscale construction typically involve divergent pathways of assembly. The numerous length scales contained within these complex structures necessitate construction pathways that are system-generated and cumulative, non-prescriptive with regard to the initial state, and highly sensitive to small changes in intrinsic and extrinsic factors (Table 1). As we have discussed, these systems typically involve temporal- and spatial-dependent coupling of several constituents that sustain and propagate the spontaneous ordering and transformation of hybrid nano-objects without the apparent intervention of any principal organizing factor. Unfortunately, such strategies are not readily amenable to systematic evaluation because of the inherent complexity associated with these emergent systems. Indeed, although progress has been made in understanding many aspects of non-equilibrium self-assembly across several length scales[99,132], there still seems to be no coherent theory of these systems.

In general, emergent structures and non-equilibrium pattern formation derive from the interplay between competitive and cooperative processes, under the imposition of local constraints, associated for example with diffusion-limited reaction fields, and maintained by energy dissipation[99,133]. The pathways show no deterministic dependence on the starting conditions or nature of the initial reactants and building blocks; instead they are contingent on many factors that together influence the type and transformation of instability thresholds in the free-energy landscape. Typically, these include symmetry breaking, microphase separation, selection pressures between various intermediates, and the interplay between collective correlations and non-equivalence in the size of the components[94]. Such nonlinear factors are highly demanding with regard to the information-generating capacity of a system, and are therefore dependent on a continuous flux and dissipation of energy to maintain complex interactions between many components. These attributes are characteristic of living systems, and it is expedient to compare the static non-equilibrium hybrid nanostructures we have described in this review with the dynamic and adaptive nature of biologically assembled materials. The latter are delicately poised in metastable states so that they can respond effectively, both structurally and functionally, to external stimuli to generate processes such as force transmission, motility, self-healing and self-replication[1]. These non-equilibrium states are maintained through biochemical networks that are displaced from equilibrium by coupling chemical reactions with diffusion-limited membrane-transport processes. In terms of a possible synthetic analogy, this would necessitate that the construction and transformation of nanoscale objects are controlled and directed by interactive linkages to a non-equilibrium chemical network that is capable of adapting to changes in environmental conditions, and feeding these back into correlated modifications in the structural and functional states of the hybrid material. For example, the coupling of an oscillating chemical reaction with a precipitation–dissolution process has been recently described[134], and Grzybowski and colleagues have suggested coupling pH-driven nanoparticle assembly with a chemical-clock reaction cycling between acidic and alkaline pH values[70]. The development of many of the processes described in this review, as well as the extension of our theoretical understanding of non-equilibrium self-assembly, will no doubt facilitate the realization of such ambitious research goals.

References

1. Mann, S. Life as a nanoscale phenomenon. *Angew. Chem. Int. Ed.* **47,** 5306–5320 (2008).
2. Shevchenko, E. V., Talapin, D. V., Kotov, N. A., O'Brien, S. & Murray, C. B. Structural diversity in binary nanoparticle superlattices. *Nature* **439,** 55–59 (2006).
3. Wang, X., Zhuang, J., Peng, O. & Li, Y. D. A general strategy for nanocrystal synthesis. *Nature* **437,** 121–124 (2005).
4. Mirkin, C. A. & Niemeyer, C. M. *Nanobiotechnology II* (Wiley-VCH, 2007).
5. Katz, E. & Willner, I. Integrated nanoparticle-biomolecule hybrid systems: synthesis, properties, and applications. *Angew. Chem. Int. Ed.* **43,** 6042–6108 (2004).
6. Girard, C., Dujardin, E., Li, M. & Mann, S. Theoretical near-field optical properties of branched plasmonic nanoparticle networks. *Phys. Rev. Letts.* **97,** 100801 (2006).
7. van Bommel, K. J. C., Friggeri, A. & Shinkai, S. Organic templates for the generation of inorganic materials. *Angew. Chem. Int. Ed.* **42,** 980–999 (2003).
8. Yamashita, I. Biosupramolecules for nano-devices: biomineralization of nanoparticles and their applications. *J. Mater. Chem.* **18,** 3813–3820 (2008).
9. Li, M., Viravaidya, C. & Mann, S. Polymer-mediated synthesis of ferritin-encapsulated inorganic nanoparticles. *Small* **3,** 1477–1481 (2007).
10. Hennequin, B. *et al.* Biocompatible, aqueous near infrared fluorescent labels based on apoferritin-encapsulated PbS quantum dots. *Adv. Mater.* **20,** 3592–3596 (2008).
11. Kramer, R. M., Li, C., Carter, D. C., Stone, M. O. & Naik, R. R. Engineered protein cages for nanomaterial synthesis. *J. Am. Chem. Soc.* **126,** 13282–13286 (2004).
12. Okuda, M. *et al.* Self-organized inorganic nanoparticle arrays on protein lattices. *Nano Lett.* **5,** 991–993 (2005).
13. Ueno, T. *et al.* Size-selective olefin hydrogenation by a Pd nanocluster provided in an apo-ferritin cage. *Angew. Chem. Int. Ed.* **43,** 2527–2530 (2004).
14. Warne, B., Kasyuich, O. I., Mayes, E. L., Wiggins, J. A. J. & Wong, K. K. W. Self assembled nanoparticulate Co: Pt for data storage applications. *IEEE Trans. Magn.* **36,** 3009–3011 (2000).
15. Aniagyei, S. E., DuFort, C., Kao, C. C. & Dragnea, B. Self-assembly approaches to nanomaterial encapsulation in viral protein cages. *J. Mater. Chem.* **18,** 3763–3774 (2008).
16. Douglas, T. & Young, M. Host–guest encapsulation of materials by assembled virus protein cages. *Nature* **393,** 152–155 (1998).
17. Liu, C. *et al.* Magnetic viruses via nano-capsid templates. *J. Magn. Magn. Mater.* **302,** 47–51 (2006).
18. Loo, L., Guenther, R. H., Lommel, S. A. & Franzen, S. Encapsidation of nanoparticles by red clover necrotic mosaic virus. *J. Am. Chem. Soc.* **129,** 11111–11117 (2007).
19. Goicochea, N. L., De, M., Rotello, V. M., Mukhopadhyay, S. & Dragnea, B. Core-like particles of an enveloped animal virus can self-assemble efficiently on artificial templates. *Nano Lett.* **7,** 2281–2290 (2007).
20. Chen, C. *et al.* Nanoparticle-templated assembly of viral protein cages. *Nano Lett.* **6,** 611–615 (2006).
21. Lu, Y. *et al.* Aerosol-assisted self-assembly of mesostructured spherical nanoparticles. *Nature* **398,** 223–226 (1999).
22. Sadasivan, S., Fowler, C. E., Khushalani, D. & Mann, S. Nucleation of MCM-41 nanoparticles by internal reorganization of disordered and nematic-like silica-surfactant clusters. *Angew. Chem. Int. Ed.* **41,** 2151–2153 (2002).
23. Perkin, K. K., Turner, J. J., Wooley, K. L. & Mann, S. Fabrication of hybrid nanocapsules by calcium phosphate mineralization of shell crosslinked polymer micelles and nanocages. *Nano Lett.* **5,** 1457–1461 (2005).
24. Jung, J. H., Ono, Y. & Shinkai, S. Novel silica structures which are prepared by transcription of various superstructures formed in organogels. *Langmuir* **16,** 1643–1649 (2000).
25. Jung, J. H., Ono, Y., Hanabusa, K. & Shinkai, S. Creation of both right-handed and left-handed silica structures by sol-gel transcription of organogel fibres comprised of chiral diaminocyclohexane derivatives. *J. Am. Chem. Soc.* **122,** 5008–5009 (2000).
26. Tamaru, S., Takeuchi, M., Sano, M. & Shinkai, S. Sol-gel transcription of sugar-appended porphyrin assemblies into fibrous silica: unimolecular stacks versus helical bundles as templates. *Angew. Chem. Int. Ed.* **41,** 853–856 (2002).
27. Meadows, P. J., Dujardin, E., Hall, S. R. & Mann, S. Template-directed synthesis of silica-coated J-aggregate nanotapes. *Chem. Commun.* 3688–3690 (2005).
28. Ono, Y. *et al.* Preparation of novel hollow fibre silica using collagen fibres as a template. *Chem. Lett.* **28,** 475–476 (1999).
29. Numata, M. *et al.* Beta-1,3-glucan polysaccharide can act as a one-dimensional host to create novel silica nanofibre structures. *Chem. Commun.* 4655–4657 (2005).
30. Ichinose, I., Hashimoto, Y. & Kunitake, T. Wrapping of bio-macromolecules (dextran, amylopectin, and horse heart cytochrome *c*) with ultrathin silicate layer. *Chem. Lett.* **33,** 656–657 (2004).
31. Patil, A. J., Muthusamy, E. & Mann, S. Synthesis and self-assembly of organoclay-wrapped biomolecules. *Angew. Chem. Int. Ed.* **43,** 4928–4933 (2004).
32. Patil, A. J., Li, M., Dujardin, E. & Mann, S. Novel bioinorganic nanostructures based on mesolamellar intercalation or single molecule wrapping of DNA using organoclay building blocks. *Nano Lett.* **7,** 2660–2665 (2007).
33. Kim, J. & Grate, J. W. Single-enzyme nanoparticles armored by a nanometer-scale organic/inorganic network. *Nano Lett.* **3,** 1219–1222 (2003).
34. Bromley, K. M., Patil, A. J., Perriman, A. W., Stubbs, G. & Mann, S. Preparation of high quality nanowires by tobacco mosaic virus templating of gold nanoparticles. *J. Mater. Chem.* **18,** 4796–4801 (2008).

35. Lemon, B. I. & Crooks, R. M. Preparation and characterization of dendrimer-encapsulated CdS semiconductor quantum dots. *J. Am. Chem. Soc.* **122,** 12886–12887 (2000).
36. Manson, C. F. & Wooley, A. T. DNA-templated construction of copper nanowires. *Nano Lett.* **3,** 359–363 (2003).
37. Behrens, S. *et al.* Nanoscale particle arrays induced by highly ordered protein assemblies. *Adv. Mater.* **14,** 1621–1625 (2002).
38. Dujardin, E., Peet, C., Stubbs, G., Culver, J. N. & Mann, S. Organization of metallic nanoparticles using tobacco mosaic virus templates. *Nano Lett.* **3,** 413–417 (2003).
39. Tseng, R. J. *et al.* Digital memory device based on tobacco mosaic virus conjugated with nanoparticles. *Nature Nanotech.* **1,** 72–77 (2006).
40. Górzny, M. L., Walton, A. S., Wnek, M., Stockley, P. G. & Evans, S. D. Four-probe electrical characterization of Pt-coated TMV-based nanostructures. *Nanotechnology* **19,** 165704 (2008).
41. Seddon, A. M., Patel, H. M., Burkett, S. L. & Mann, S. Chiral templating of silica-lipid lamellar mesophase with helical tubular architecture. *Angew. Chem. Int. Ed.* **41,** 2988–2991 (2002).
42. Chappel, J. S. & Yager, P. Formation of mineral microstructures with a high aspect ratio from phospholipid bilayer tubules. *J. Mater. Sci. Lett.* **11,** 633–636 (1992).
43. Yuwono, V. M. & Hartgerink, J. D. Peptide amphiphile nanofibres template and catalyse silica nanotube formation. *Langmuir* **23,** 5033–5038 (2007).
44. Hartgerink, J. D., Beniash, E. & Stupp, S. I. Self-assembly and mineralization of peptide-amphiphile nanofibres. *Science* **294,** 1684–1688 (2001).
45. Wang, H. *et al.* Cylindrical block co-micelles with spatially selective functionalization by nanoparticles. *J. Am. Chem. Soc.* **129,** 12924–12925 (2007).
46. Wang, H. *et al.* Fabrication of continuous and segmented polymer/metal oxide nanowires using cylindrical micelles and block co-micelles as templates. *Adv. Mater.* **21,** 1805–1808 (2009).
47. Sone, E. D., Zubarev, E. R. & Stupp, S. I. Semiconductor nanohelices templated by supramolecular ribbons. *Angew. Chem. Int. Ed.* **41,** 1705–1709 (2002).
48. Sone, E. D., Zubarev, E. R. & Stupp, S. I. Supramolecular templating of single and double nanohelices of cadmium sulphide. *Small* **5,** 694–697 (2005).
49. Perkin, K. K., Hirsch, A., Böttcher, C. & Mann, S. Nanoscale organization and patterning of cadmium sulphide quantum dots on structurally persistent dendro-calixarene micelles. *Small* **3,** 2057–2060 (2007).
50. Yu, L. T., Banerjee, I. A., Shima, M., Rajan, K. & Matsui, H. Size-controlled Ni nanocrystal growth on peptide nanotubes and their magnetic properties. *Adv. Mater.* **16,** 709–712 (2004).
51. Banerjee, I. A., Yu, L. T. & Matsui, H. Cu nanocrystal growth on peptide nanotubes by biomineralization: size control of Cu nanocrystals by tuning peptide conformation. *Proc. Natl Acad. Sci. USA* **100,** 14678–14682 (2003).
52. Reches, M. & Gazit, E. Casting metal nanowires within discrete self-assembled peptide nanotubes. *Science* **300,** 625–627 (2003).
53. Meegan, J. E. *et al.* Designed self-assembled beta-sheet peptide fibrils as templates for silica nanotubes. *Adv. Funct. Mater.* **14,** 31–37 (2004).
54. Holmström, S. C. *et al.* Templating silica nanostructures on rationally designed self-assembled peptide fibres. *Langmuir* **24,** 11778–11783 (2008).
55. Schnur, J. M. Lipid tubules: A paradigm for molecularly engineered structures. *Science* **262,** 1669–1676 (1993).
56. Yan, X. H., Liu, G. J., Haeussler, M. & Tang, B. Z. Water-dispersible polymer/Pd/Ni hybrid magnetic nanofibres. *Chem. Mater.* **17,** 6053–6059 (2005).
57. Duxin, N., Liu, F. T., Vali, H. & Eisenberg, A. Cadmium sulphide quantum dots in morphologically tunable triblock copolymer aggregates. *J. Am. Chem. Soc.* **127,** 10063–10069 (2005).
58. Kellermann, M. *et al.* The first account of a structurally persistent micelle. *Angew. Chem. Int. Ed.* **43,** 2959–2962 (2004).
59. Sadasivan, S., Dujardin, E., Li, M., Johnson, C. J. & Mann, S. DNA-driven assembly of mesoporous silica/gold satellite nanoparticles. *Small* **1,** 103–106 (2005).
60. Mirkin, C. A., Letsinger, R. L., Mucic, R, C. & Storhoff, J. J. DNA-based method for rationally assembling nanoparticles into macroscopic materials. *Nature* **382,** 607–609 (1996).
61. Niemeyer, C. M. Nanoparticles, proteins, and nucleic acids: Biotechnology meets materials science. *Angew. Chem. Int. Ed.* **40,** 4128–4158 (2001).
62. Li, M., Dujardin, E. & Mann, S. Programmed assembly of multi-layered protein/nanoparticle-carbon nanotube conjugates. *Chem. Commun.* 4952–4954 (2005).
63. Ishii, D. *et al.* Chaperonin-mediated stabilization and ATP-triggered release of semiconductor nanoparticles. *Nature* **423,** 628–632 (2003).
64. Scheibel, T. *et al.* Conducting nanowires built by controlled self-assembly of amyloid fibres and selective metal deposition. *Proc. Natl Acad. Sci. USA* **100,** 4527–4532 (2003).
65. Medalsy, I *et al.* SP1 protein-based nanostructures and arrays. *Nano Lett.* **8,** 473–477 (2008).
66. Gottlieb, D., Morin, S. A., Jin, S. & Raines, R. T. Self-assembled collagen-like peptide fibres as templates for metallic nanowires. *J. Mater. Chem.* **18,** 3865–3870 (2008).
67. Wang, Q., Lin, T., Tang, L., Johnson, J. E. & Finn, M. G. Icosahedral virus particles as addressable nanoscale building blocks. *Angew. Chem. Int. Ed.* **41,** 459–462 (2002).
68. McMillan, R. A. *et al.* Ordered nanoparticle arrays formed on engineered chaperonin protein templates. *Nature Mater.* **1,** 247–252 (2002).
69. Patolsky, F., Weizmann, Y. & Willner, I. Actin-based metallic nanowires as bio-nanotransporters. *Nature Mater.* **3,** 692–695 (2004).
70. Grybowski, B. A., Wilmer, C. E., Kim, J., Browne, K. P. & Bishop, K. J. M. Self-assembly: from crystals to cells. *Soft Matter* **5,** 1110–1128 (2009).
71. Sun, J. *et al.* Core-controlled polymorphism in virus-like particles. *Proc. Natl Acad. Sci. USA* **104,** 1354–1359 (2007).
72. Kalsin, A. M. *et al.* Electrostatic self-assembly of binary nanoparticle crystals with a diamond lattice. *Science* **312,** 420–424 (2006).
73. Nykypanchuk, D., Maye, M. M., van der Lelie, D. & Gang, O. DNA-guided crystallization of colloidal nanoparticles. *Nature* **451,** 549–552 (2008).
74. Park, S. Y. *et al.* DNA-programmable nanoparticle crystallization. *Nature* **451,** 553–556 (2008).
75. Tlusty, T. & Safran, S. A. Defect-induced phase separation in dipolar fluids. *Science* **290,** 1328–1331 (2000).
76. Tang, Z. Y., Kotov, N. A. & Giersig, M. Spontaneous organization of single CdTe nanoparticles into luminescent nanowires. *Science* **297,** 237–240 (2002).
77. Lin, S., Li, M., Dujardin, E., Girard, C. & Mann, S. One-dimensional plasmon coupling by facile self-assembly of gold nanoparticles into branched chain networks. *Adv. Mater.* **17,** 2553–2559 (2005).
78. DeVries, G. A. *et al.* Divalent metal nanoparticles. *Science* **315,** 358–361 (2007).
79. Adams, M., Dogic, Z., Keller, S. L. & Fraden, S. Entropically driven microphase transitions in mixtures of colloidal rods and spheres. *Nature* **393,** 349–352 (1998).
80. Nikoobakht, B., Wang, Z. L. & El-Sayed, M. A. Self-assembly of gold nanorods. *J. Phys. Chem. B* **104,** 8635–8640 (2000).
81. Puntes, V. F., Krishnan, K. M. & Alivisatos, A. P. Colloidal nanocrystal shape and size control: the case of cobalt. *Science* **291,** 2115–2117 (2001).
82. Li, M., Schnablegger, H. & Mann, S. Coupled synthesis and self-assembly of nanoparticles to give structures with controlled organization. *Nature* **402,** 393–395 (1999).
83. Nie, Z. *et al.* Self-assembly of metal–polymer analogues of amphiphilic triblock copolymers. *Nature Mater.* **6,** 609–614 (2007).
84. Stankovich, S. *et al.* Stable aqueous dispersions of graphitic nanoplatelets *via* the reduction of exfoliated graphite oxide in the presence of poly(sodium 4-styrenesulfonate). *J. Mater. Chem.* **16,** 155–158 (2006).
85. Patil, A. J., Vickery, J. L., Scott, T. B. & Mann, S. Aqueous stabilization and self-assembly of graphene sheets into layered bio-nanocomposites using DNA. *Adv. Mater.* **21,** 3159–3164 (2009).
86. Penn, R. L. & Banfield, J. F. Morphology development and crystal growth in nanocrystalline aggregates under hydrothermal conditions: insights from titania. *Geochim. Cosmochim. Acta* **63,** 1549–1557 (1999).
87. Coelfen, H. & Antonietti, M. Mesocrystals: inorganic superstructures made by highly parallel crystallization and controlled alignment. *Angew. Chem. Int. Ed.* **44,** 5576–5591 (2005).
88. Coelfen, H. & Mann, S. Higher-order organization by mesoscale self-assembly and transformation of hybrid nanostructures. *Angew. Chem. Int. Ed.* **42,** 2350–2365 (2003).
89. Mann, S. The chemistry of form. *Angew. Chem. Int. Ed.* **39,** 3392–3406 (2000).
90. Simon, P. *et al.* On the real-structure of biomimetically grown hexagonal prismatic seeds of fluorapatite-gelatine-composites: TEM investigations along [001]. *J. Mater. Chem.* **14,** 2218–2224 (2004).
91. Yu, S.-H., Coelfen, H., Tauer, K. & Antonietti, M. Tectonic arrangement of $BaCO_3$ nanocrystals into helices induced by a racemic block copolymer. *Nature Mater.* **4,** 51–55 (2005).
92. Wang, T. X., Coelfen, H. & Antonietti, M. Nonclassical crystallization: mesocrystals and morphology change of $CaCO_3$ crystals in the presence of a polyelectrolyte additive. *J. Am. Chem. Soc.* **127,** 3246–3247 (2005).
93. Busch, S. *et al.* Biomimetic morphogenesis of fluorapatite-gelatin composites: fractal growth, the question of intrinsic electric fields, core/shell assemblies, hollow spheres and reorganization of denatured collagen. *Eur. J. Inorg. Chem.* 1643–1653 (1999).
94. Ball, P. *The Self-Made Tapestry: Pattern Formation in Nature* (Oxford Univ. Press, 1999).
95. Li, M. & Mann, S. Emergent hybrid nanostructures based on non-equilibrium block copolymer self-assembly. *Angew. Chem. Int. Ed.* **47,** 9476–9479 (2008).
96. Backov, R. Combining soft matter and soft chemistry: integrative chemistry towards designing novel and complex multiscale architectures. *Soft Matter* **2,** 452–464 (2006).
97. Chandrappa, G. T., Steunou, N. & Livage, J. Macroporous crystalline vanadium oxide foam. *Nature* **416,** 702 (2002).
98. Walsh, D. *et al.* Preparation of higher-order zeolite materials using dextran templating. *Angew. Chem. Int. Ed.* **43,** 6691–6695 (2004).

99. Grzybowski, B. A., Bishop, K. J. M., Campbell, C. J., Fialkowski, M. & Smoukov, S. K. Micro- and nanotechnology via reaction-diffusion. *Soft Matter* **1,** 114–128 (2005).
100. Nicolis, G. & Prigogine, I. *Self-Organization in Nonequilibrium Systems - From Dissipative Structures to Order Through Fluctuations* (Wiley, 1977).
101. Haase, C. S., Chadam, J., Feinn, D. & Ortoleva, P. Oscillatory zoning in plagioclase feldspar. *Science* **209,** 272–274 (1980).
102. Short, M. B. *et al.* Stalactite growth as a free-boundary problem: a geometric law and its platonic ideal. *Phys. Rev. Lett.* **94,** 18501 (2005).
103. Tabor, Z., Rokita, E. & Cichocki, T. Origin of the pattern of trabecular bone: an experiment and a model. *Phys. Rev. E* **66,** 51906 (2002).
104. Liesegang, R. E. Uber einige Eigenschaften von Gallerten. *Naturwiss. Wochenschr.* **11,** 353–362 (1896).
105. Devon, R., RoseFigura, J., Douthat, D., Kudenov, J. & Maselko, J. Complex morphology in a simple chemical system. *Chem. Commun.* 1678–1680 (2005).
106. Collins, A. M., Carriazo, D., Davis, S. A & Mann, S. Spontaneous template-free assembly of ordered macroporous titania. *Chem Commun.* 568–569 (2004).
107. Leonard, A. & Su, B. L. A novel and template-free method for the spontaneous formation of aluminosilicate macro-channels with mesoporous walls. *Chem. Commun*. 1674–1675 (2004).
108. Deng, W. H. & Shanks, B. H. Synthesis of hierarchically structured aluminas under controlled hydrodynamic conditions. *Chem. Mater*. **17,** 3092–3100 (2005).
109. Henisch, H. K. *Crystals in Gels and Liesegang Rings* (Cambridge Univ. Press, 1988).
110. Mueller, K. F. Periodic interfacial precipitation in polymer films. *Science* **225,** 1021–1027 (1984).
111. Bitner, A., Fialkowski, M., Smoukov, S. K., Campbell, C. J. & Grzybowski, B. A. Amplification of changes of a thin film's macromolecular structure into macroscopic reaction–diffusion patterns. *J. Am. Chem. Soc.* **127,** 6936–6937 (2005).
112. Sugawara, A., Ishii, T. & Kato, T. Self-organized calcium carbonate with regular surface-relief structures. *Angew. Chem. Int. Ed.* **42,** 5299–5303 (2003).
113. Imai, H., Tatar, S., Furuichi, K. & Oaki, Y. Formation of calcium phosphate having a hierarchically laminated architecture through periodic precipitation in organic gel. *Chem. Commun.* 1952–1953 (2003).
114. Voinescu, A. E. *et al.* Inorganic self-organized silica aragonite biomorphic composites. *Cryst. Growth Des.* **8,** 1515–1521 (2008).
115. Yu, J., Guo, H., Davis, S. A. & Mann, S. Fabrication of monodisperse calcium carbonate hollow microspheres by chemically induced self-transformation. *Adv. Funct. Mater.* **16,** 2035–2041 (2006).
116. Zeng, H. C. Synthetic architecture of interior space for inorganic nanostructures. *J. Mater. Chem*. **16,** 649–662 (2006).
117. Oaki, Y. & Imai, H. Hierarchically organized superstructure emerging from the exquisite association of inorganic crystals, organic polymers, and dyes: a model approach towards suprabiomineral materials. *Adv. Funct. Mater.* **15,** 1407–1414 (2005).
118. Li, M., Coelfen, H. & Mann, S. Morphological control of $BaSO_4$ microstructures by double hydrophilic block copolymer mixtures. *J. Mater. Chem*. **14,** 2269–2276 (2004).
119. Viravaidya, C., Li, M. & Mann, S. Microemulsion-based synthesis of stacked calcium carbonate (calcite) superstructures. *Chem Commun.* 2182–2183 (2004).
120. Xing, Y., Li, M., Davis, S. A. & Mann, S. Synthesis and characterization of cerium phosphate nanowires in microemulsion reaction media. *J. Phys. Chem.* **110,** 1111–1113 (2006).
121. Aisenberg, J., Miller, D. A., Grazul, J. L. & Hamann, D. R. Direct fabrication of large micropatterned single crystals. *Science* **299,** 1205–1208 (2003).
122. Nakanishi, T. *et al.* Flower-shaped supramolecular assemblies: hierarchical organization of a fullerene bearing long aliphatic chains. *Small* **3,** 2019–2023 (2007).
123. Garcia-Ruiz, J. M., Melero-Gracia, E. & Hyde, S. T. Morphogenesis of self-assembled nanocrystalline materials of barium carbonate and silica. *Science* **323,** 362–365 (2009).
124. Escudero, C., Crusats, J., Diez-Perez, I., El-Hachemi, Z. & Ribó, J. Folding and hydrodynamic forces in J-aggregates of 5-phenyl-10,15,20-tris (4-sulphophenyl)porphyrin. *Angew. Chem. Int. Ed.* **45,** 8032–8035 (2006).
125. Hopwood, J. D. & Mann, S. Synthesis of barium sulphate nanoparticles and nanofilaments in reverse micelles and microemulsions. *Chem. Mater.* **9,** 1819–1828 (1997).
126. Klajn, R., Bishop, K. J. M. & Grzybowski, B. A. Light-controlled self-assembly of reversible and irreversible nanoparticle suprastructures. *Proc. Natl Acad. Sci. USA* **104,** 10305–10309 (2007).
127. Bruinsma, R. F., Gelbart, W. M., Reguera, D., Rudnick, J. & Zandi, R. Viral self-assembly as a thermodynamic process. *Phys. Rev. Lett.* **90,** 248101 (2003).
128. Israelachvili, J. *Intermolecular & Surface Forces* (Academic Press, 1991).
129. Mann, S. *Biomineralization: Principles and Concepts in Bioinorganic Materials Chemistry* (Oxford Univ. Press, 2001).
130. Lee, S. Y., Royston, E., Culver, J. & Harris, M. Improved metal cluster deposition on a genetically engineered tobacco mosaic virus template. *Nanotechnology* **16,** S435–S441 (2005).
131. Douglas, T. *et al.* Protein engineering of a viral cage for constrained nanomaterials synthesis. *Adv. Mater.* **14,** 415–418 (2002).
132. Grzybowski, B. A. & Campbell, C. J. Complexity and dynamic self-assembly. *Chem. Eng. Sci.* **59,** 1667–1676 (2004).
133. Cross, M. C. & Hohenberg, P. C. Pattern formation out of equilibrium. *Rev. Mod. Phys.* **65,** 851–1112 (1993).
134. Kurin-Csorgei, K., Epstein, I. R. & Orban, M. Systematic design of chemical oscillators using complexation and precipitation equilibria. *Nature* **433,** 139–142 (2005).